



Contents lists available at ScienceDirect

## Materials Today: Proceedings

journal homepage: [www.elsevier.com/locate/matpr](http://www.elsevier.com/locate/matpr)

# The use of back surface field and passivation layer to enhance the performance of silicon heterojunction solar cells

Venkanna Kanneboina\*, Hemambika Sadasivuni

Department of Science and Humanities, St. Martin's Engineering College, Secunderabad, Telangana 500100, India

## ARTICLE INFO

Article history:  
Available online xxxxx

Keywords:  
Back surface field  
Simulation  
Passivation  
Silicon heterojunction solar cells

## ABSTRACT

c-Si/a-Si:H heterojunction solar cells (Si-HJSCs) are simulated by AFORS-HET to study their performance with the back surface field (BSF) and passivation layer. Si-HJSCs (*ninip*) with the best open circuit voltage ( $V_{oc}$ ) (760.8 V), short circuit current density ( $J_{sc}$ ) (36.97 mA/cm<sup>2</sup>), fill factor ( $FF$ ) (85.22%), and efficiency ( $\eta$ ) (24.17%) were achieved. Whereas, estimated values of 675.2 mV, 33.5 mA/cm<sup>2</sup>, 83.34%, and 18.98% for a basic Si-HJSC (*np*) SC, which corresponds to the  $V_{oc}$ ,  $J_{sc}$ ,  $FF$  and  $\eta$ . The intrinsic -a-Si:H layer on both sides of the c-Si wafer has passivated the dangling bond density on the silicon, and the defect density at the interface between the c-Si and a-Si:H layers and improved the performance of Si-HJSCs. These simulation results were compared with experimental data for accuracy and validation. It was observed that the simulation results are highly promising and almost match experimental data.

Copyright © 2023 Elsevier Ltd. All rights reserved.

Selection and peer-review under responsibility of the scientific committee of the 2nd International Conference on Multifunctional Materials.

## 1. Introduction

In a homojunction, the band gap is formed between materials with the same band gap, while in a heterojunction, the band gap is formed between materials with different band gaps [1]. Recombination losses are decreased by the heterojunction due to the separation of carriers moving in opposite directions [2,3]. In a result, the photocurrent produced by the SC is increased [4]. By improving surface passivation and reducing charge carrier recombination, silicon HJSCs can generate better  $V_{oc}$  and  $\eta$  than c-Si SCs. The conversion  $\eta$  is like that of c-Si SCs when it comes to turning sunlight into energy [5–7].

In 1974, the a-Si/c-Si HJSC was reported initially by Fuhs et al. [8]; the a-Si/poly c-Si HJSC was reported by Okuda et al. in 198 with an  $\eta$  of 12% [9]. In 1992, Sanyo introduced its cutting-edge silicon HJSC PV technology, which has since reached an  $\eta$  of 18.1% [10]. Heterojunction with intrinsic thin layer (HIT) SHJSCs use an i-a-Si:H layer inserted between the c-Si and doped a-Si:H layers to generate a heterojunction. Passivation of the c-Si interface and surface is accomplished by utilizing this layer [10]. Many groups are currently studying Si-HJSCs with the goal of improving efficiency of solar cell [11–15].

The effectiveness of Si-HJSCs was studied here by employing the AFORS-HET modelling software. The performance of Si-HJSCs was evaluated by measuring their efficiency, quantum efficiency, and spectrum responses. Simulated results were compared with experimental data for validation and correctness.

## 2. Details of simulation

AFORS-HET is used for modelling Si-HJSCs. Different configurations of Si-HJSCs are shown in Fig. 1(a-c). Reliable references are used for the density of states distribution, layer density and thermal velocity in all layers and other parameters [17–19,22–28]. The remaining parameters in AFORS-HET are used with their default settings [16,20,21,24].

## 3. Results and discussion

### 3.1. J-V characteristics of Silicon HJSCs

Current density against voltage (J-V) for Si-HJSCs is shown in Fig. 2. Silicon HJSC performance was evaluated in three different setups, as indicated in Fig. 2.  $V_{oc}$ ,  $J_{sc}$ ,  $FF$ , and  $\eta$  of the estimated SC properties shown in Table 1. A fixed 5 nm thick a-Si:H layer was used throughout. These a-Si:H layers having a constant band-gap value. The ITO layer thickness of these SCs is only 70 nm. The

\* Corresponding author.

E-mail address: [venkanna@alumni.iitg.ac.in](mailto:venkanna@alumni.iitg.ac.in) (V. Kanneboina).

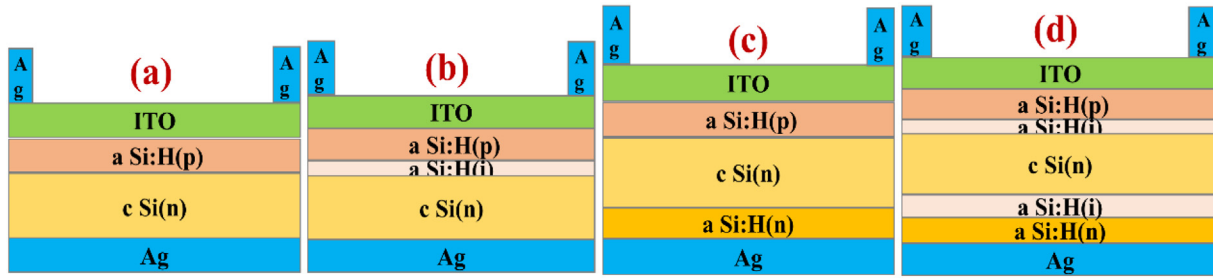


Fig. 1. Schematic structure a) *np*, b) *nip*, c) *nnp*, d) *ninip* of Si-HJSCs.

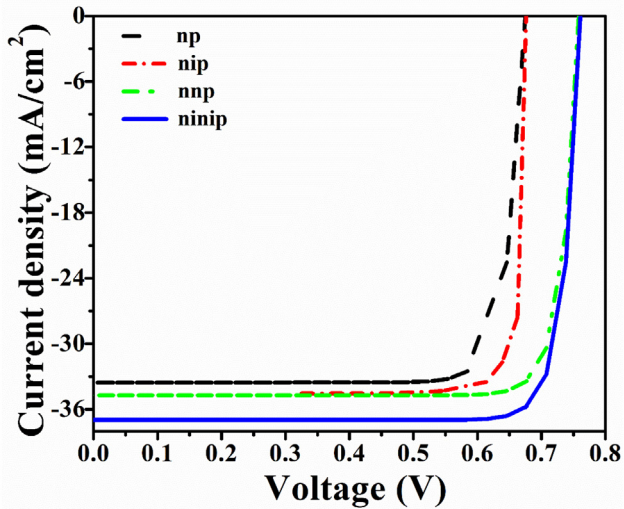


Fig. 2. Current density of SCs measured with voltage.

$V_{oc}$  of 675.2 V,  $J_{sc}$  of 33.53 mA/cm<sup>2</sup>,  $FF$  of 83.34%, and  $\eta$  of 18.98% are the computed parameters for a *np* solar cell (Fig. 1a) (Table 1). Due to a high recombination density and many dangling bonds, c-Si wafers have an extremely low  $V_{oc}$  and  $J_{sc}$ . There is a loss of  $\eta$  because the internal electric field is weak at the semiconductor junction, charge carriers recombine, and fewer e-h's collected at Ag contacts. Incorporating an intrinsic passivation layer (Fig. 1b) somewhat improves the solar cell characteristics (Table 1). In the *nnp* structure, the n-a-Si:H BSF is superimposed on the *np* structure (Fig. 1c). Table 1 shows that the *nnp* solar cell has a  $V_{oc}$  of 757.9 V, a  $J_{sc}$  of 34.71 mA/cm<sup>2</sup>, an  $FF$  of 85.85%, and an  $\eta$  of 22.62%. Fig. 2 displays the enhanced  $V_{oc}$  and  $J_{sc}$  of 757.9 V and 34.71 mA/cm<sup>2</sup> for *nnp* SCs with n-a-Si:H BSF layers. The improved electric field at the junction is mostly due to the BSF's ability to reduce recombination losses. The i-a-Si:H layer has been implanted on both the top and bottom of the c-Si wafer to boost the electric field across the junction (Fig. 1d). Along with increasing the electric field at the junction, this i-a-Si:H layers also serve to passivate dangling bonding density on the surface of c-Si and the interface between c-Si and the p-a-Si:H/n-a-Si:H layer [29–32]. While both  $V_{oc}$  and  $J_{sc}$  have increased, the  $FF$  has remained relatively unchanged. A value of

24.17% is attained by SCs with a *ninip* structure, i-a-Si:H passivation layer, and a BSF.

### 3.2. Si-HJSCs: Spectral response

Fig. 3 depicts the Si-HJSC's spectral response (SR) for the wavelengths 300–1200 nm. The SR of *ninip* SCs increased steadily with wavelength, from 30% at 350 nm to 71% at 950 nm. The *nnp* SCs have a somewhat lower spectrum response than *ninip* SCs. At 1000 nm, the SR% dropped to 30%, and at 1100 nm, it dropped to practically nil, without any discernible change in intensity. The spectral response of *np* SCs has been reduced by around 10% to 12% from 800 to 1050 nm. Applying a BSF and covering silicon HJSCs with a thinner i-a-Si:H may improve their spectrum responsiveness.

### 3.3. Si-HJSCs: Quantum efficiency

The external quantum efficiency (EQE) of Si-HJSCs is shown in Fig. 4 to be between 300 and 1200 nm. For *np* SCs, 80% EQE is located between 350 and 900 nm. When compared to *np* SCs, the external quantum of *ninip* and *nnp* SCs is larger in the 350–1100 nm range. For *ninip* SCs, the EQE is closest to 85% at 430 nm, somewhat lower at 550 nm, and gradually increasing at 950 nm. Improvements in spectral performance between 350 and 450 nm may be seen when comparing spectra from *np* and *nip* cells. In the same way, the EQE of *nnp* SCs has dropped by about 2% between 400 and 1000 nm. The *ninip* and *nnp* SCs are more costly but have better EQE spectra than *np* SCs. When a passivation layer and BSF are applied to SCs, the EQE significantly increases.

In Fig. 5 depicts internal quantum efficiency (IQE) Si-HJSCs. The number of internal quantum fluctuations is proportional to the number of free charge carriers captured per incident photon. The *np* SCs have an IQE of around 80% between 350 and 900 nm. In comparison to *np* SCs, the IQE of *ninip* and *nnp* SCs is increased around 350–1100 nm. Improvements in spectral performance between 350 and 450 nm may be seen when comparing spectra from *np* and *nip* cells. The *ninip* SCs obtain about 87% IQE at 430 nm, somewhat less at 550 nm, and gradually more at 950 nm. The EQE spectrum is narrower and less strong than the IQE spectrum when it comes to *ninip*, *nnp*, and *np* SCs. When a passivation layer and BSF are applied to SCs, the IQE significantly increases.

## 4. Experimental validation

Table 2 displays the results of a comparison between the simulated SCs, and the experimental reports used to validate the simulations. We have previously reported that we have successfully built n-type wafer-based single-sided c-Si/a-Si:H HJ (*nip*) structured SCs with an  $\eta$  of 17.3% [30]. The simulation results for *nip* structured SCs were found to be slightly higher than the experimental values. It is also observed that the results are very encour-

Table 1  
Solar cell characteristics of Si-HJSCs.

Structures	$V_{oc}$ (mV)	$J_{sc}$ (mA/cm <sup>2</sup> )	$FF$ (%)	$\eta$ (%)
<i>np</i>	675.2	33.53	83.34	18.98
<i>nip</i>	676.3	34.54	83.91	19.62
<i>nnp</i>	757.9	34.71	85.85	22.62
<i>ninip</i>	760.8	36.97	85.92	24.17

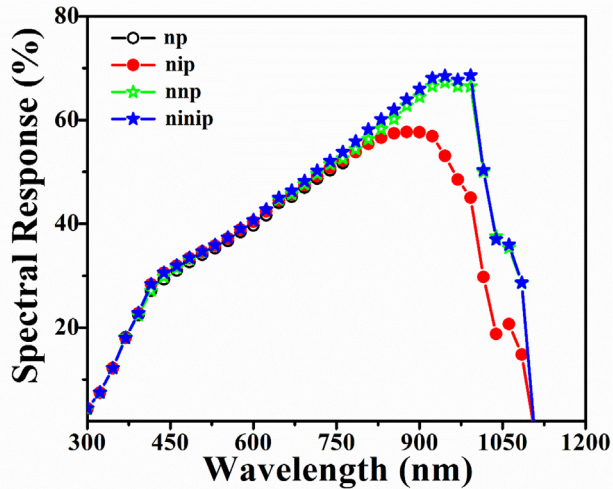


Fig. 3. SR of SCs measured by wavelength.

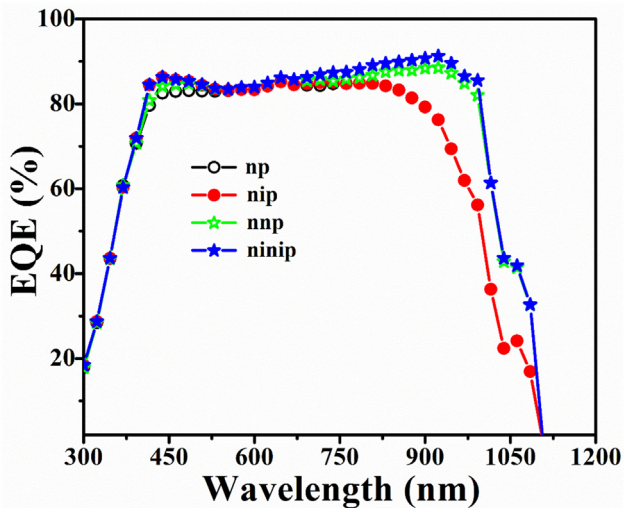


Fig. 4. EQE of SCs as a function of wavelength.

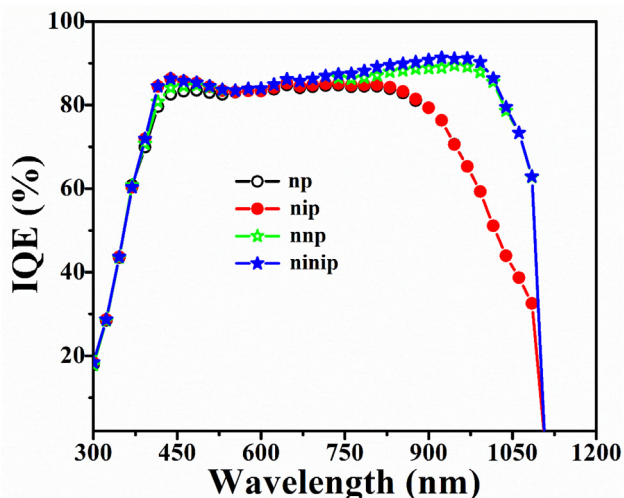


Fig. 5. IQE of SCs as a function of wavelength.

Table 2

Characteristics of simulated and experimental Si-HJSCs.

Structures	$V_{oc}$ (mV)	$J_{sc}$ (mA/cm <sup>2</sup> )	FF(%)	$\eta$ (%)
*nip (Simulation)	676.3	34.54	83.91	19.62
#nip (Experimental)	705	32.72	75	17.30 [30]
*nnp (Simulation)	760.8	36.97	85.92	24.17
ninip (Experimental)	750	39.50	83.2	24.70 [33]
ninip (Experimental)	740	41.80	82.7	25.60 [6]

(\* this work; # our previously reported work).

aging and nearly matching with experimental results when compared the results from simulated cells of *ninip* structured Si-HJSCs to those from the reported work.

## 5. Conclusions

Performance of the different structured Si-HJSCs have been studied by AFORS-HET tool. The BSF and passivation layer were added to the Si-HJSCs to assess its performance. High  $V_{oc}$  of 760.8 V,  $J_{sc}$  of 36.97 mA/cm<sup>2</sup>, FF of 85.22% and  $\eta$  of 24.17% were achieved with *ninip* SCs. It is observed that SC parameter values are 757.9 mV, 34.71 mA/cm<sup>2</sup>, 85.85 % and 22.62 % corresponding to  $V_{oc}$ ,  $J_{sc}$ , FF and  $\eta$  for *nnp* SCs. A basic *np* solar cell is expected to have an  $V_{oc}$  of 675 mV, an  $J_{sc}$  of 33.53 mA/cm<sup>2</sup>, FF and an  $\eta$  of 83.44% and 18.98% respectively. There has been a significant increase in the performance of *ninip* SCs owing to the extremely thin layer of a-Si:H on both sides of c-Si that passivates most of the dangling bonding density and interface defect density. The internal electric field at the junction was enhanced by adding sufficient BSF with n-a-Si:H layer to separate free charge carriers and rapidly access metal contacts. This electric field with n-a-Si:H significantly reduced recombination density at the interface. It was found that these simulation results are highly promising and almost match experimental results.

## CRedit authorship contribution statement

**Venkanna Kanneboina:** Conceptualization, Methodology, Software, Data curation, Writing – original draft, Investigation, Writing – review & editing. **Hemambika Sadasivuni:** Writing – review & editing.

## Data availability

Data will be made available on request.

## Declaration of Competing Interest

The authors declare that they have no known competing financial interests or personal relationships that could have appeared to influence the work reported in this paper.

## References

- [1] S.M. Sze, Semiconductor Devices Physics and Technology, 3rd Edition, Wiley. (2017). 10.1007/978-3-319-63154-7.
- [2] T.F. Schulze, L. Korte, F. Ruske, B. Rech, Band lineup in amorphous/crystalline silicon heterojunctions and the impact of hydrogen microstructure and topological disorder, Phys. Rev. B 83 (2011) 1–11, <https://doi.org/10.1103/PhysRevB.83.165314>.
- [3] L. Korte, E. Conrad, H. Angermann, R. Stangl, M. Schmidt, Advances in a-Si:H/c-Si heterojunction solar cell fabrication and characterization, Solar Energy Materials and SCs. 93 (2009) 905–910, <https://doi.org/10.1016/j.solmat.2008.10.020>.
- [4] L.K. Wilfried, G.J. H.M.van Sark, Physics and technology of amorphous-crystalline heterojunction silicon SCs, 2012. 10.1007/978-3-642-22275-7.
- [5] J. Zhao, A. Wang, M.A. Green, High- $\eta$  PERL and PERT silicon SCs on FZ and MCZ substrates, Solar Energy Materials and SCs. 65 (2001) 429–435, [https://doi.org/10.1016/S0927-0248\(00\)00123-9](https://doi.org/10.1016/S0927-0248(00)00123-9).

- [6] K. Masuko, M. Shigematsu, T. Hashiguchi, D. Fujishima, M. Kai, N. Yoshimura, T. Yamaguchi, Y. Ichihashi, T. Mishima, N. Matsubara, T. Yamanishi, T. Takahama, M. Taguchi, E. Maruyama, S. Okamoto, Achievement of More Than 25% Conversion  $\eta$  With Crystalline Silicon Heterojunction Solar Cell, *IEEE J. Photovoltaics* 4 (2014) 1433–1435, <https://doi.org/10.1109/JPHOTOV.2014.2352151>.
- [7] M.A. Green, Y. Hishikawa, A.W.Y.H. Baillie, E.D. Dunlop, D.H. Levi, Solar cell  $\eta$  tables (version 51), *Prog. Photovolt. Res. Appl.* 26 (2018) 3–12, <https://doi.org/10.1002/ppp.2978>.
- [8] W. Fuhs, K. Niemann, J. Stuke, Heterojunctions of Amorphous Silicon and Silicon Single Crystals, *AIP Conf. Proc.* 20 (1974) 345–350, <https://doi.org/10.1063/1.2945985>.
- [9] Y.H. Kojji Okudu, H. Okamoto, Amorphous Si Polycrystalline Si Stacked Solar Cell Having More Than 12% Conversion  $\eta$ , *Jpn. J. Appl. Phys.* 9 (1983) 605–607, <https://doi.org/10.1143/JJAP.22.L605>.
- [10] M. Tanaka, M. Taguchi, T. Matsuyama, T. Sawada, S. Tsuda, S. Nakano, H. Hanafusa, Y. Kuwano, Development of New a-Si/C-Si HJSCs: ACJ-HIT (Artificially Constructed Junction-Heterojunction With Intrinsic Thin-Layer), *Japanese Journal of Applied Physics Part 1-Regular Papers Short Notes & Review Papers*. 31 (1992) 3518–3522, <https://doi.org/10.1143/JJAP.31.3518>.
- [11] S.W.G.J. Benick, R. Müller, F. Schindler, A. Richter, H. Hauser, F. Feldmann, P. Krenckel, S. Riepe, M.C. Schubert, M. Hermle, Approaching 22%  $\eta$  with multicrystalline n-type silicon SCs, *PV Solar Energy Conference and Exhibition*. 33 (2017) 1188–1197.
- [12] S. De Wolf, A. Descoedres, Z.C. Holman, C. Ballif, High- $\eta$  Silicon HJSCs: A Review, *Green*. 2 (2012) 7–24, <https://doi.org/10.1515/green-2011-0018>.
- [13] B. Zhang, Y. Zhang, R. Cong, Y. Li, W. Yu, G. Fu, Superior silicon surface passivation in HIT SCs by optimizing a-SiO<sub>x</sub>: H thin films: A compact intrinsic passivation layer, *Sol. Energy* 155 (2017) 670–678, <https://doi.org/10.1016/j.solener.2017.06.066>.
- [14] Y. Liu, Y. Li, Y. Wu, G. Yang, L. Mazzarella, P. Procel-Moya, A.C. Tamboli, K. Weber, M. Boccard, O. Isabella, X. Yang, B. Sun, High- $\eta$  Silicon HJSCs: Materials, Devices and Applications, *Mater. Sci. Eng. R. Rep.* 142 (2020), <https://doi.org/10.1016/j.mser.2020.100579>.
- [15] J. Zhou, Q. Huang, Y. Ding, G. Hou, Y. Zhao, Passivating contacts for high- $\eta$  silicon-based SCs: From single-junction to tandem architecture, *Nano Energy* 92 (2022), <https://doi.org/10.1016/j.nanoen.2021.106712>.
- [16] R. Varache, C. Leendertz, M.E. Gueunier-Farret, J. Haschke, D. Muñoz, L. Korte, Investigation of selective junctions using a newly developed tunnel current model for solar cell applications, *Solar Energy Materials and SCs*. 141 (2015) 14–23, <https://doi.org/10.1016/j.solmat.2015.05.014>.
- [17] L. Zhao, C.L. Zhou, H.L. Li, H.W. Diao, W.J. Wang, Design optimization of bifacial HIT SCs on p-type silicon substrates by simulation, *Solar Energy Materials and SCs*. 92 (2008) 673–681, <https://doi.org/10.1016/j.solmat.2008.01.018>.
- [18] X. Wen, X. Zeng, W. Liao, Q. Lei, S. Yin, An approach for improving the carriers transport properties of a-Si:H/c-Si HJSCs with  $\eta$  of more than 27%, *Sol. Energy* 96 (2013) 168–176, <https://doi.org/10.1016/j.solener.2013.07.019>.
- [19] S. Singh, S. Kumar, N. Dwivedi, Band gap optimization of p-i-n layers of a-Si: H by computer aided simulation for development of efficient solar cell, *Sol. Energy* 86 (2012) 1470–1476, <https://doi.org/10.1016/j.solener.2012.02.007>.
- [20] R. Stangl, M. Kriegel, M. Schmidt, AFORS-HET, version 2.2, a numerical computer program for simulation of HJSCs and measurements, Conference Record of the 2006 IEEE 4th World Conference on Photovoltaic Energy Conversion, WCPEC-4. 2 (2007) 1350–1353. 10.1109/WCPEC.2006.279681.
- [21] R. Stangl, M. Kriegel, K. V. Maydell, L. Korte, M. Schmidt, W. Fuhs, AFORS-HET, an open-source on demand numerical PC program for simulation of (thin film) HJSCs, version 1.2, Conference Record of the IEEE Photovoltaic Specialists Conference. (2005) 1556–1559. 10.1109/PVSC.2005.1488441.
- [22] Y. Ide, Y. Saito, A. Yamada, M. Konagai, 2-Step Growth Method and Microcrystalline Silicon Thin Film SCs Prepared by Hot Wire Cell Method, *Jpn. J. Appl. Phys.* 43 (2004) 2419–2424, <https://doi.org/10.1143/JJAP.43.2419>.
- [23] R. Stangl, C. Leendertz, J. Haschke, Numerical Simulation of SCs and Solar Cell Characterization Methods : the Open-Source on Demand Program AFORS-HET (2010), <https://doi.org/10.5772/8073>.
- [24] N. Dwivedi, S. Kumar, A. Bisht, K. Patel, S. Sudhakar, Simulation approach for optimization of device structure and thickness of HIT SCs to achieve  $\sim 27\%$   $\eta$ , *Sol. Energy* 88 (2013) 31–41, <https://doi.org/10.1016/j.solener.2012.11.008>.
- [25] Y. Yao, X. Xu, X. Zhang, H. Zhou, X. Gu, S. Xiao, Enhanced  $\eta$  in bifacial HIT SCs by gradient doping with AFORS-HET simulation, *Mater. Sci. Semicond. Process.* 77 (2018) 16–23, <https://doi.org/10.1016/j.mssp.2018.01.009>.
- [26] Stephen J Fonash, *Solar cell device physics*, Elsevier. (2010). 10.1016/0025-5408(82)90173-8.
- [27] R.E.I. Schropp, M. Zeman, *Amorphous and Microcrystalline Silicon SCs: Modeling, Materials and Device Technology* (1998), <https://doi.org/10.1007/978-1-4615-5631-2>.
- [28] S.M. Iftiqar, H. Park, S. Kim, J. Yi, Theoretical investigation of transparent front surface field layer on the performance of heterojunction silicon solar cell, *Solar Energy Materials and SCs*. 204 (2020), <https://doi.org/10.1016/j.solmat.2019.110238>.
- [29] Venkanna Kanneboina, Ramakrishna Madaka, P. Agarwal, High open circuit voltage Si-HJSCs: Influence of hydrogen plasma treatment studied by spectroscopic ellipsometry, *Solar Energy*. 166 (2018) 255–266. 10.1016/j.solener.2018.03.068.
- [30] R. Venkanna Kanneboina, P.A. Madaka, Stepwise tuning of the doping and thickness of p-a-Si: H emitter layer to improve the performance of c-Si(n)/p-a-Si:HHJSCs, *J. Mater. Sci. Mater. Electron.* 32 (2021) 4457–4465, <https://doi.org/10.1007/s10854-020-05187-5>.
- [31] V. Kanneboina, R. Madaka, P. Agarwal, Spectroscopic ellipsometry studies on microstructure evolution of a-Si: H to nc-Si: H films by H<sub>2</sub> plasma exposure, *Mater Today Commun.* 15 (2018) 18–29, <https://doi.org/10.1016/j.mtcomm.2018.02.023>.
- [32] R. Madaka, D. Kumar, A.K. Singh, M.d. Seraj Uddin, J. Kumar Rath, Tunnel recombination junction influence on the a-Si:H/SHJ tandem solar cell, *Mater Today Proc.* 39 (2021) 1970–1973, <https://doi.org/10.1016/j.matpr.2020.08.451>.
- [33] M. Taguchi, A. Yano, S. Tohoda, K. Matsuyama, Y. Nakamura, T. Nishiwaki, K. Fujita, E. Maruyama, 24.7% Record  $\eta$  HIT solar cell on thin silicon wafer, *IEEE J. Photovoltaics* 4 (2014) 96–99, <https://doi.org/10.1109/JPHOTOV.2013.2282737>.